Heat Mass Transfer
DOI 10.1007/s00231-012-1043-5

ORIGINAL

A comparative analysis of various shaped film-cooling holes

Sun-Min Kim · Ki-Don Lee · Kwang-Yong Kim

Received: 5 July 2011 / Accepted: 18 June 2012

Abstract In the present work, numerical analysis has been performed to investigate the film-cooling performance of various film-cooling hole schemes such as fan, crescent, louver, and dumbbell-shaped holes. To analyze the turbulent flow and the film-cooling mechanism, three-dimensional Reynolds-averaged Navier–Stokes analysis has been performed with the shear stress transport turbulence model. The validation of the numerical results for the film-cooling effectiveness has been performed in comparison with experimental data. The film-cooling performance for each hole shape has been evaluated in terms of the centerline, laterally averaged, and spatially averaged film-cooling effectiveness values. The dumbbell-shaped hole shows the best spatially averaged film-cooling effectiveness for all blowing ratios tested in this work.

List of symbols

D Film-cooling hole diameter
M Blowing ratio ($=\rho_j U_j/\rho_m U_m$)
R Radius
U Velocity (m/s)
ρ Density (kg/m^3)
T Temperature (K)
η Film-cooling effectiveness

Subscripts/superscripts

aw Adiabatic wall
m Main hot gas
s Spatially averaged value
j Coolant jet
c Centerline on the cooling surface
l Laterally averaged value

S.-M. Kim · K.-D. Lee · K.-Y. Kim (✉)
Department of Mechanical Engineering,
Inha University, 253 Yonghyun-Dong,
Nam-Gu, Incheon 402-751, Republic of Korea
e-mail: kykim@inha.ac.kr

1 Introduction

The inlet temperature of the turbine stage has been increased to obtain high efficiency and low fuel consumption in gas turbines. Accordingly, the thermal and mechanical loads on the component exposed to hot gas have been increased as well; thus, an extremely efficient cooling technique is necessitated. Film cooling is one of the major technologies to cool blades down in gas turbines. In this technique, a coolant is blown over the surface exposed to hot gas and a film of low-temperature gas protects the metal surface from the hot gas. Because of the high importance of film cooling, considerable research on various shapes of film-cooling hole have been performed in the last 10–15 years.

The effectiveness of film cooling depends on a variety of parameters such as the blowing ratio, density ratio, main stream turbulence intensity, momentum flux ratio, and geometrical parameters such as the inclination angle, injection angle, diffuser angle, diameter of holes, etc. But most of all, those for the film-cooling hole geometry are the most influential parameters regarding film-cooling performance. Therefore, various film-cooling hole schemes have been developed over the past few decades to increase the cooling performance. Bunker [1] studied and reviewed various shapes of film-cooling hole. The purpose of these film-cooling holes is to increase the effectiveness by reducing the penetration of coolant into the main stream and extending the exit area for a wide spread over the cooling surface. Heidmann and Ekkad [2] introduced the antivortex hole that is made with the intention of

Published online: 01 July 2012

counteracting the detrimental vortices associated with standard circular cross-sectioned film-cooling holes. Taslim and Ugarte [3] studied the discharge coefficient through compound-angle conical and cylindrical holes. A conical hole has a higher discharge coefficient than a cylindrical hole under high pressure; both shapes tend to show greater discharge coefficients when the directions of the main stream and the coolant are the same.

Lu [4] carried out both experimental and numerical analyses to evaluate the film-cooling effectiveness, heat transfer coefficient, and heat flux for crescent, converging slot, trench, cratered, cylindrical, and diffuser shaped film-cooling holes. In this study, the crescent hole yielded higher film-cooling effectiveness than the converging slot hole and extremely higher than the cylindrical hole. And, the cratered hole showed lower film-cooling effectiveness than the diffuser shaped hole. Hyams and Leylek [5] performed computational simulations to investigate the velocity ratio, path line, vorticity distribution, and film-cooling effectiveness for cylindrical, forward-diffused, laterally-diffused, inlet, and cusp shaped holes. They reported that the cusp hole has lower effectiveness than the lateral diffuser hole. Newly shaped holes named dumbbell and bean holes were developed by Liu et al. [6]. The film-cooling performance for the newly shaped holes was evaluated by comparison with cylindrical and fan shaped holes, and the dumbbell-shaped hole showed higher effectiveness overall than the fan and bean shaped holes. Yu et al. [7] measured and compared the film-cooling effectiveness, heat transfer coefficient, and heat flux ratio for cylindrical and forward diffused cylindrical holes, and forward and lateral diffused cylindrical holes. A hybrid hole scheme was introduced by Ghorab et al. [8]. In this study, the net heat flux reduction on the cooling surface, Frossling number, and film-cooling effectiveness for the hybrid hole were compared with those of cylindrical and fan shaped holes, and the hybrid hole showed the highest film-cooling effectiveness.

A novel film-cooling scheme named the louver hole was introduced by Zhang and Hassan [9], who evaluated its film-cooling effectiveness by comparison with cylindrical and console holes. The louver hole showed better film-cooling performance near the exit, but lower performance far from the hole exit compared to the console hole. Sargison et al. [10] studied the characteristics regarding the film-cooling effectiveness, heat transfer coefficient, and aerodynamic loss for cylindrical, fan, slot, and console shaped holes. The slot and console holes showed better film-cooling effectiveness and heat transfer coefficients than the cylindrical and fan shaped holes. Nasir et al. [11] investigated the effect of the orientation of the triangular tabs for the cylindrical hole on the film-cooling performance. The film holes with tabs showed higher film-cooling effectiveness due to the generation of secondary eddies that counter-rotated with respect to the pair of kidney vortices. Lu et al. [12] investigated the effects of the width and depth of the trench on film cooling effectiveness for cylindrical holes. They reported that the cylindrical hole with a trench shows less film-cooling performance than the fan shaped hole. Liu et al. [13] studied the waist-shaped slot hole. The waist-shaped slot hole showed subnormal film-cooling effectiveness in comparison with the conventional slot hole.

As mentioned above, there are a variety of shapes of film-cooling hole, and most of them include a cylindrical part at the bottom. However, not many of the reported investigations have compared the flow mechanism and film-cooling performance for various hole shapes. Therefore, the main purpose of the present study is to analyze the flow characteristics and measure the film-cooling effectiveness for various hole shapes that are known to yield high cooling performance. But additional devices such as trenches or tabs were not considered due to the range of applicable hole shapes. The louver, fan, crescent, and dumbbell shapes of hole have been selected for comparison through Reynolds-averaged Navier–Stokes (RANS) analysis for various blowing ratios, viz., M = 0.5, 1.0, 1.5 and 2.0.

2 Numerical analysis

Three-dimensional RANS analysis of the fluid flow and heat transfer is conducted by using ANSYS CFX-11.0 [14], which utilizes an unstructured grid system. The solutions are obtained by solving the compressible RANS equations through the finite-volume method to discretize the governing differential equations. The shear stress transport (SST) turbulence model [15, 16] that incorporates the advantages of both the k-ε and k-ω models was used as the turbulence closure.

The shapes of film-cooling hole are shown in Fig. 1. In the present work, the film-cooling performance of four different shaped film-cooling holes, viz., crescent [4], dumbbell [6], louver [8], and fan shaped holes [1], has been numerically analyzed and compared for the same boundary conditions. For the boundary conditions and computational domain, the experimental environment of Saumweber et al. [17] was referred; it is well known for good validity and also has been cited by many researchers. And, all the holes were set to the same dimensions regarding the hole diameter (D = 5 mm), hole pitch (6D), main channel (270 mm × 30 mm × 41 mm), and plenum (100 mm × 30 mm × 20 mm).

Figure 2 shows the computational domain with dimensions and boundary conditions. The geometry of the computational domain was created by the software ANSYS 11.0 Design Modeler. The working fluid was ideal gas (air).

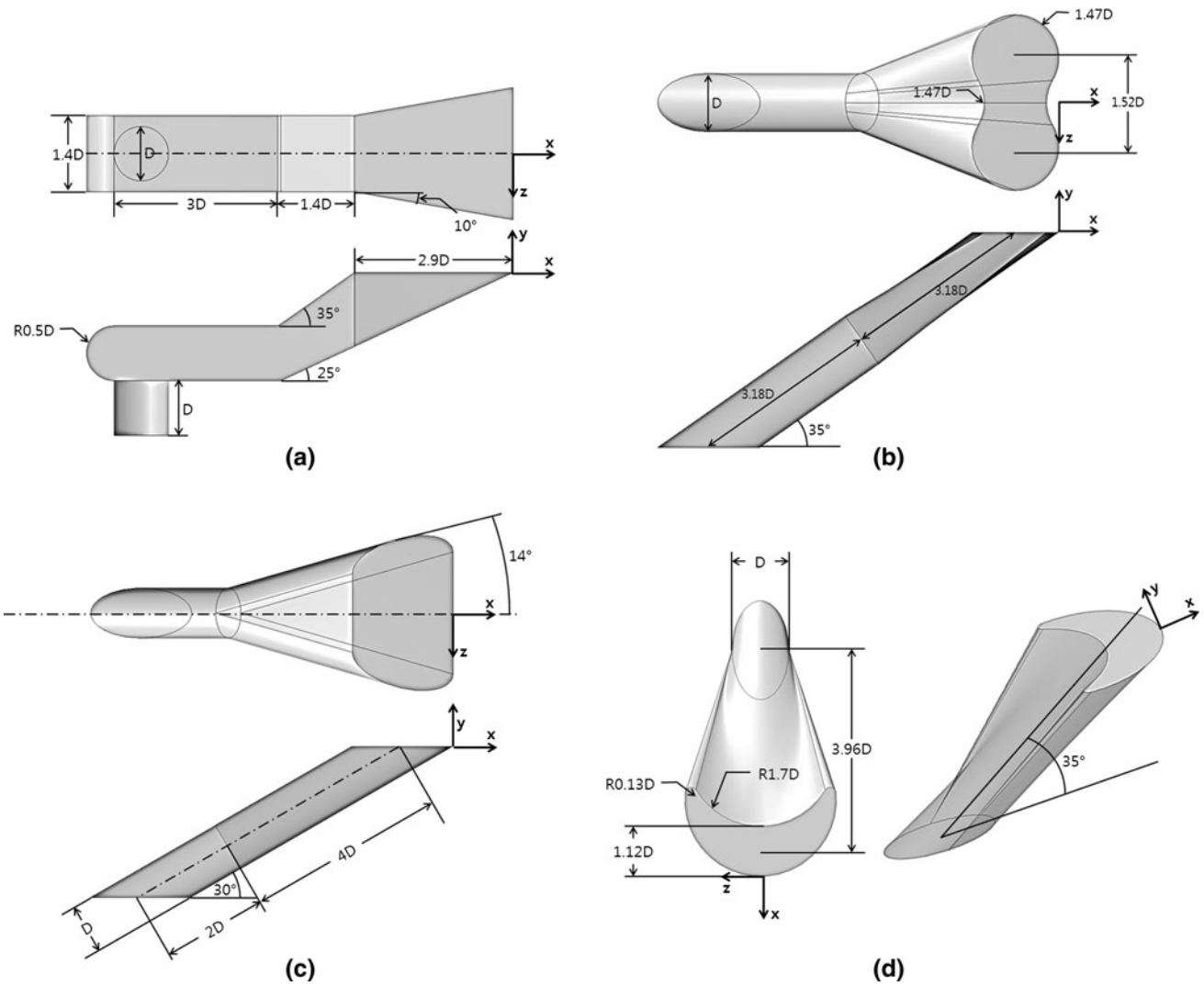

Fig. 1 Selected shapes of film-cooling hole: **a** louver, **b** dumbbell, **c** fan, and **d** crescent

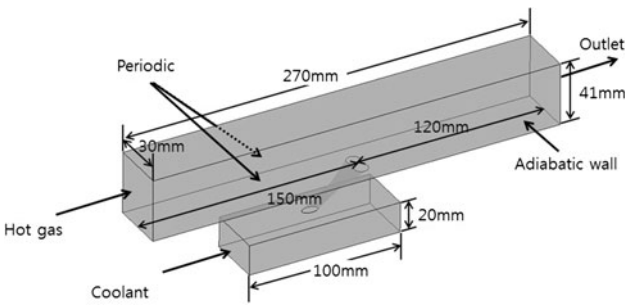

Fig. 2 Computational domain

The inlet boundary condition for the second (coolant) flow was a mass flow rate of 0.0033 kg/s at a temperature of 290 °K. And, the inlet boundary condition for the main flow was modeled with a normal speed of 139 m/s at a temperature of 540 °K and a turbulence intensity of 3.5 %. The outlet condition was a constant static pressure of 1 atm. The walls were constructed with the no-slip and adiabatic conditions. And, the periodic conditions are applied at the side boundaries of the computational domain to reflect the periodicity of the holes.

The meshes that were created by ANSYS ICEM CFD-11.0 were made up of tetrahedral grids, and an example of the computational grid for the louver-shaped hole is shown in Fig. 3. To increase the accuracy of calculation near the walls, a prism mesh was used at the wall of the film-cooling hole and the cooling surface. In order to find out the optimal number of computational nodes, four different grid systems with number of nodes ranging from about 300,000 to 5,500,000 were tested, and an example of test results for the louver shaped hole is shown in Fig. 4. From the results, about 1.6, 1.4, 1.7, and 1.4 million nodes were selected as the optimum numbers of nodes for the crescent,

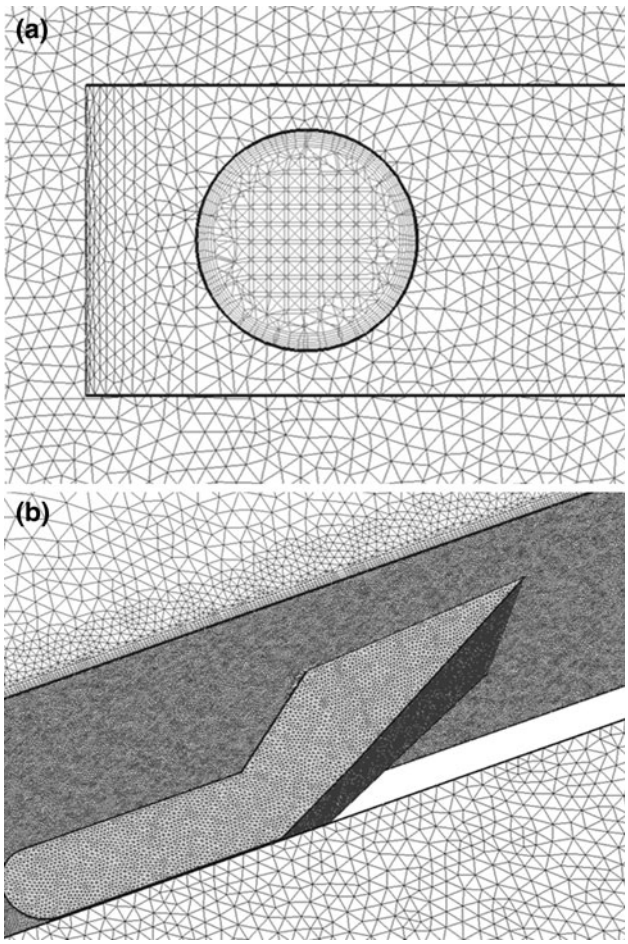

Fig. 3 An example of computational grids (louver hole): **a** *bottom* view of the hole. **b** Cooling surface and hole

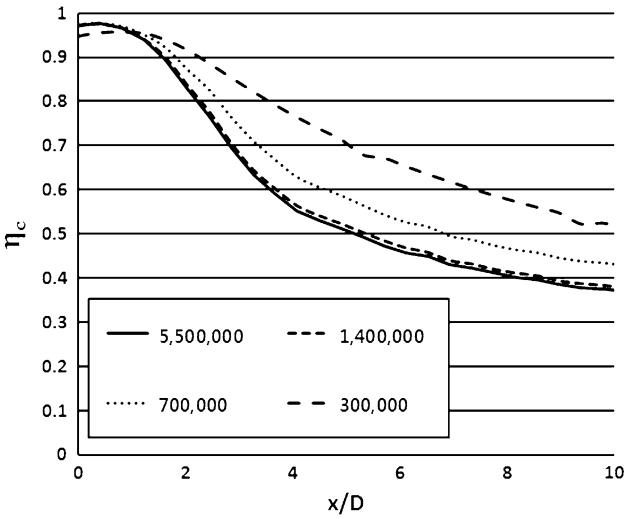

Fig. 4 An example of grid test (dumbbell hole)

dumbbell, louver, and fan shaped holes, respectively. The first grid points from the wall were placed in the range (0.005–0.02 mm) to satisfy the values of y+ less than 2. Inside the hole, owing to complex flow phenomena, the technique of limiting the size of the mesh was applied to have size of 0.5 mm for detailed analysis. The bottom of the main channel is the surface where the coolant and hot gas meet together; therefore, there was also a limitation in terms of the mesh size (0.1–0.2 mm), but in this case, the size of the mesh increased at a constant ratio from the wall.

Regarding the convergence criteria, the RMS relative residual values of all the flow parameters were set to 1.0E−5. The computations were performed using an Intel Core i7 CPU K 875 @2.93 GHz. The computational time per single analysis was about 20–25 h, and the time was dependent on the complexity of the geometry and the number and quality of meshes, etc.

3 Results and discussion

To assess the validity of the numerical solutions, the results were compared with experimental data for the louver, fan and crescent shaped film-cooling holes under the same boundary conditions with the corresponding experiments [4, 9, 17] as shown in Fig. 5. The geometric conditions, such as diameter and pitch of hole, etc., for each shaped hole follow their own experimental environment. First of all, to find appropriate turbulence model, the comparison among four turbulence closure models, viz, standard k-ε model [18], k-ω model [16], SST model [15], and RNG k-ε model [19], was carried out for the louver shaped hole as shown in Fig. 5a. The CFD results with the SST model shows best agreements (averaged error of 2.85 %) with the experimental data among the tested models. And, the standard k-ε model shows large over prediction on the film-cooling effectiveness. Therefore, further calculations were performed using the SST model. Figure 5b shows the laterally averaged film-cooling effectiveness for the fan and crescent shaped hole. The laterally averaged effectiveness means effectiveness value which is averaged along the line transverse to the x-direction on the cooling surface. This laterally averaged film-cooling effectiveness indicates how the coolant spreads laterally at specific position. The film-cooling effectiveness is the parameter used by many researchers to evaluate the performance of film cooling, and is defined as follows:

$$\eta = (T_{\text{hot}} - T_{\text{aw}})/(T_{\text{hot}} - T_{\text{coolant}}) \quad (1)$$

where T_{aw} indicates the temperature at the adiabatic wall, and T_{hot}, T_{coolant} are the temperatures of the main stream and coolant, respectively. As shown in Fig. 5b, the results for the fan-shaped hole showed some deviation from the experimental data near the hole (x/D $\leq$ 5), but showed good agreement downstream of x/D = 5.0 with average

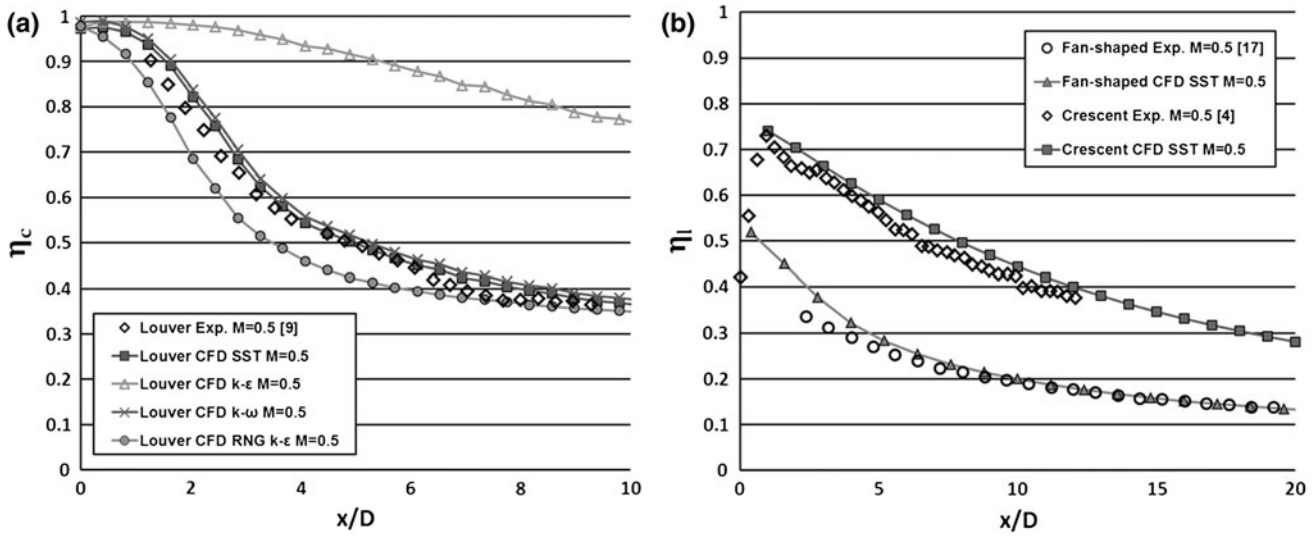

Fig. 5 Validation of computational results for the film-cooling effectiveness: **a** film-cooling effectiveness at the centerline for the louver-shaped hole. **b** Laterally averaged film-cooling effectiveness for the fan-shaped hole

error of 2.94 %. In the case of the crescent hole, the numerical results show little over prediction, but generally good agreements with the experimental data over the entire cooling surface with relative errors in the range, 1–8 %. Overall, the present numerical results agree reasonably well with the experimental data.

The contours of the local film-cooling effectiveness on the cooling surface for the crescent, dumbbell, louver, and fan-shaped holes are showed for various blowing ratios in Fig. 6. When the blowing ratio is 0.5, the coolant flows issuing from the shaped holes generally tend to narrowly distribute on the cooling surface compared to the case of higher blowing ratios. The crescent-shaped hole yields extremely wide, lateral spreading of coolant but very low film-cooling effectiveness at the central region of the film-cooling surface, and this causes poor cooling performance. And, two thin branches are shown in the results for the crescent-shaped hole. In contrast to the crescent-shaped hole, the louver-shaped hole shows a narrower spread of coolant for higher blowing ratios, and three big branches develop just downstream of the hole exit regardless of the blowing ratio. At first glance, the dumbbell and fan shaped holes show a larger area of high film effectiveness compared to the other shapes.

The centerline film-cooling effectiveness that demonstrates the adhesiveness of the coolant to the blade

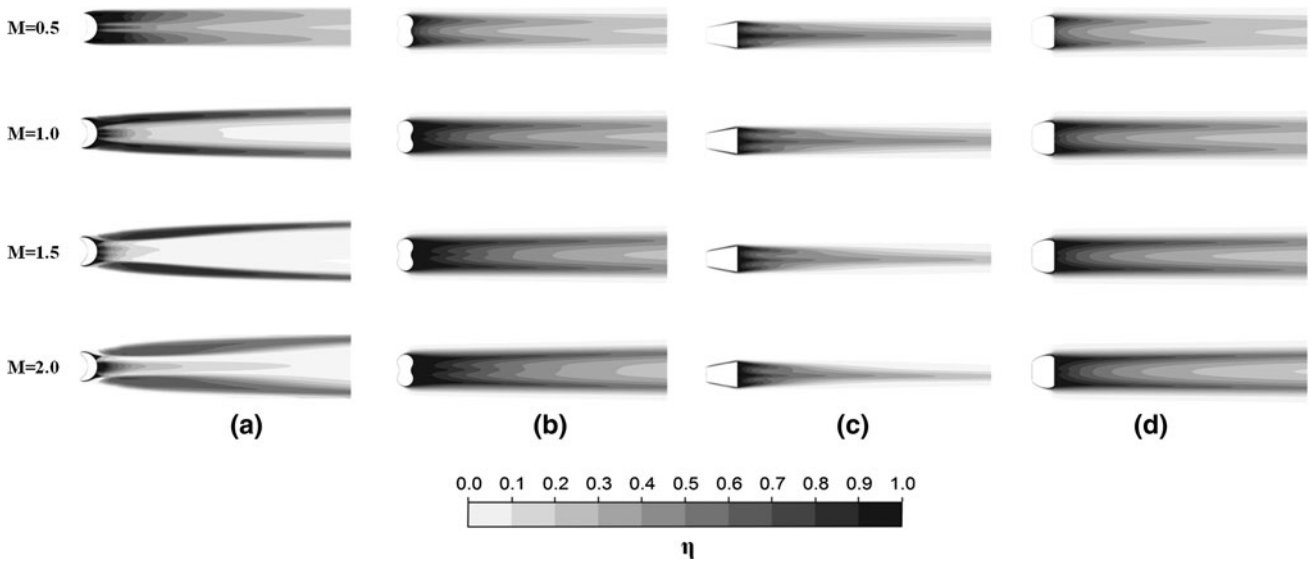

Fig. 6 Contours of the film-cooling effectiveness for various blowing ratios: **a** crescent, **b** dumbbell, **c** louver, and **d** fan

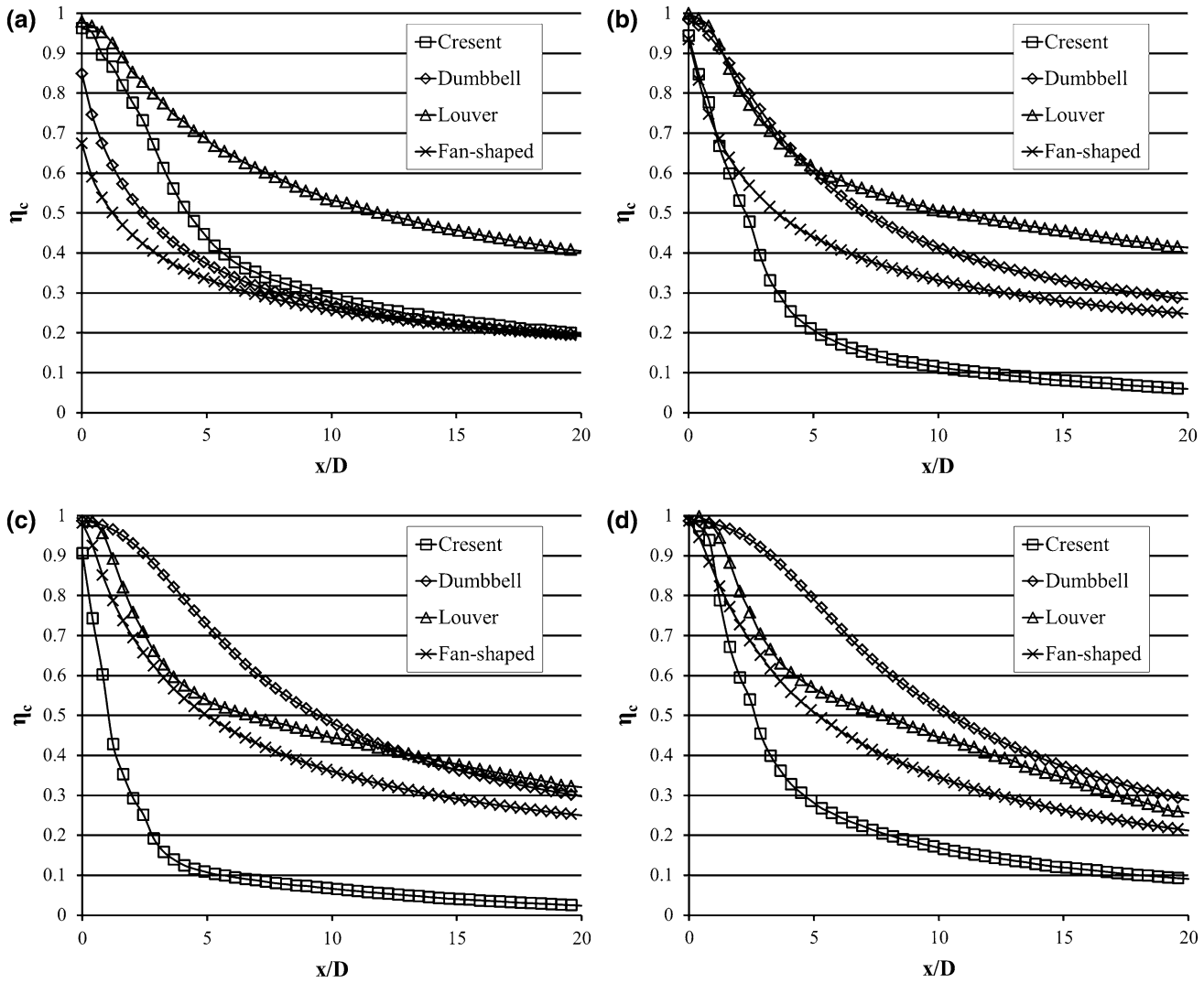

Fig. 7 The centerline film-cooling effectiveness for various blowing ratios: **a** M = 0.5, **b** M = 1.0, **c** M = 1.5, and **d** M = 2.0

surface along the streamwise direction for the four hole shapes is shown in Fig. 7. At M = 0.5, the fan-shaped and dumbbell holes start from lower values than others. These two holes show two main branches aside of the centerline and the absence of coolant at the centerline near the hole exit. As the blowing ratio increases, the coolants for the dumbbell and fan-shaped holes have increased adhesiveness on the centerline. The higher blowing ratio makes small branch at the centerline, and this make the centerline film-cooling effectiveness higher. The crescent hole shows lower centerline film-cooling effectiveness until blowing ratio reaches at 1.5. This tendency have a change at M = 2.0 by making branch at the centerline. The film-cooling effectiveness distributions for the louver hole show no significant change at all blowing ratios. At M = 0.5 and 1.0, the louver-shaped hole shows the highest film-cooling effectiveness throughout the domain. This is due to the characteristics of the louver-shaped hole, which induces high concentration along the centerline and this lasts for a long distance. But, at M = 1.5 and 2.0, the dumbbell shaped hole shows the highest centerline film-cooling effectiveness. This phenomenon is caused by the central branch that develops between the two main branches, but this branch is not found at lower blowing ratios, viz., M = 0.5 and 1.0, as shown in Fig. 6.

Figure 8 shows distributions of the laterally averaged film-cooling effectiveness for a range of the blowing ratio of 0.5–2.0. At M = 0.5, the crescent shaped hole shows the highest laterally averaged film-cooling effectiveness, while the louver shaped hole shows the highest centerline film-cooling effectiveness, as shown in Fig. 7. However, the dumbbell hole shows the highest values for both the laterally averaged and the central film-cooling effectiveness at M = 1.5 and 2.0. This indicates that the dumbbell hole yields a relatively uniform distribution for the film-cooling

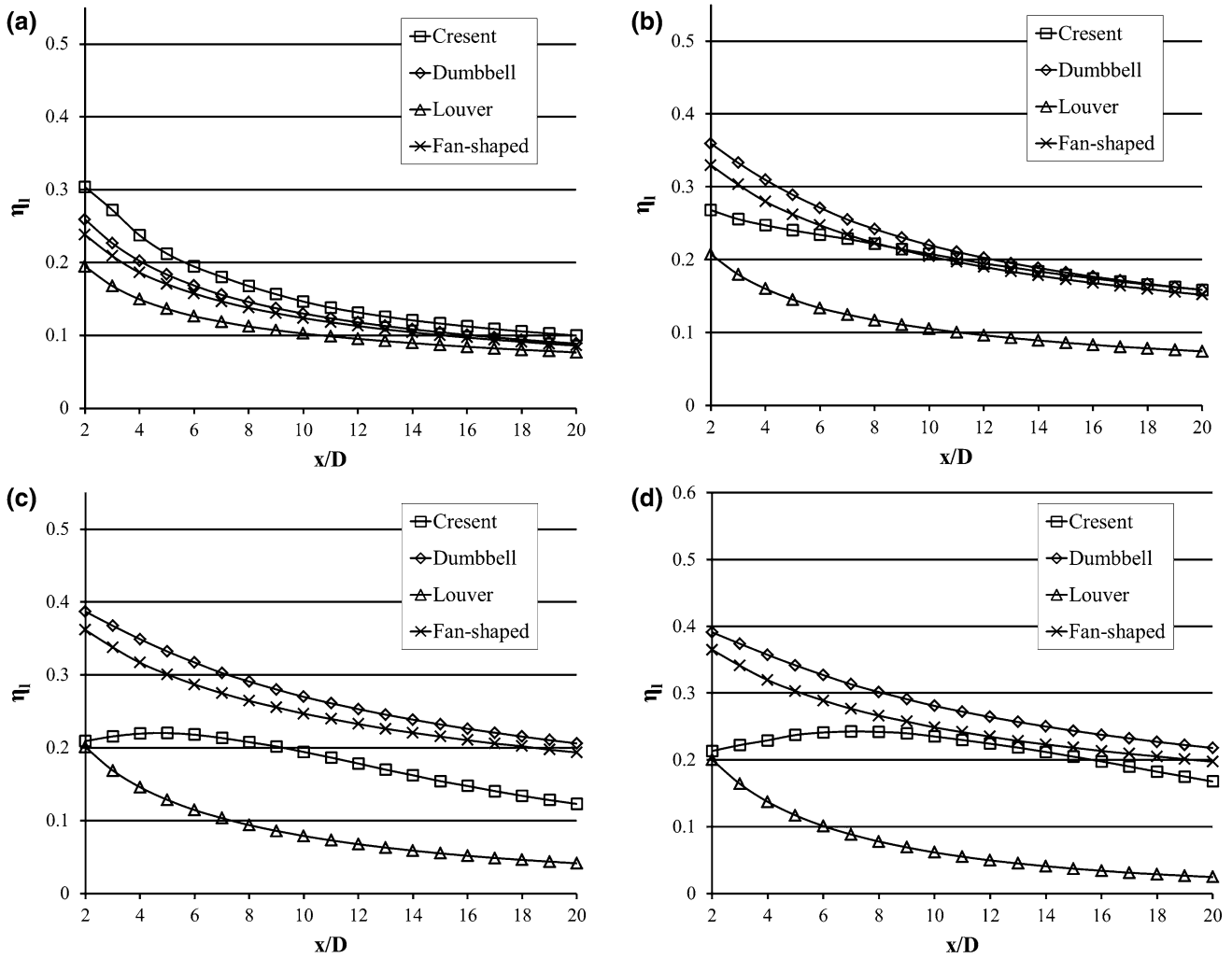

Fig. 8 The laterally averaged film-cooling effectiveness for various blowing ratios: **a** M = 0.5, **b** M = 1.0, **c** M = 1.5, and **d** M = 2.0

effectiveness in the lateral direction. As the blowing ratio increases, the crescent shaped hole widens the space between the two main coolant branches, and there exist a few footprints of coolant in the central region as shown in Fig. 6. This makes the crescent shaped hole have a lower laterally averaged film-cooling effectiveness at higher blowing ratios. At M = 2.0, quantities of coolant have more penetration into the mainstream, and this make the adhesiveness of coolant on the cooling surface weak. Therefore, when the blowing ratio is changed from 1.5 to 2.0, all kinds of hole show more or less similar laterally averaged film-cooling effectiveness.

The front and side views of the streamlines inside the hole are shown in Figs. 9 and 10, respectively. As shown in Fig. 9a, the crescent shaped hole makes the coolant spread out to the outside. This is induced by strong impingement of the coolant on the upper wall of the hole (Fig. 10a). A small part of the coolant is blown out with screwing along the centerline, but most of the coolant is spread laterally by a pushing force that is induced by the strong impingement. The dumbbell shaped hole also makes the coolant spread out. But, the coolant does not spread widely unlike the case of the crescent hole as shown in Fig. 9b. And, the impingement of coolant is weaker than that in the crescent shaped hole at the upper wall of the hole (Fig. 10b). In the louver shaped hole, a strong recirculating zone is generated at the corner by the impingement of the flow on the upper horizontal wall of the hole as shown in Fig. 10c, and the coolant flow is divided into two strong streams after the impingement, which are concentrated along the centerline as the jet issues from the hole as shown in Fig. 9c. But, unlike the crescent shaped hole, the impingement of coolant at the upper wall is weak. The fan shaped hole shows a flow structure that is similar to that of the dumbbell shaped hole as shown in Fig. 9d. But, in the fan shaped hole, the flow separation occurs on the bottom wall of the diffuser part as shown in Fig. 10d due to the shape of the hole;

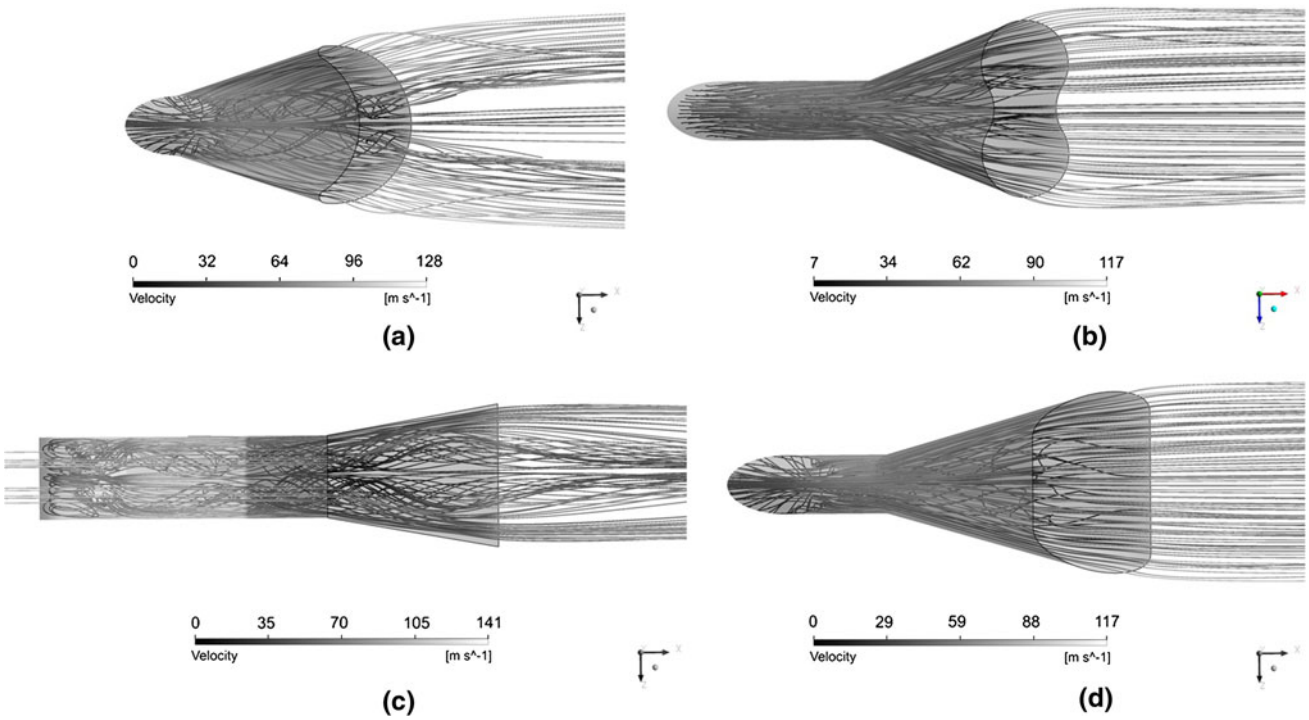

Fig. 9 Streamlines inside the hole (*top view*, M = 0.5): **a** crescent, **b** dumbbell, **c** louver, and **d** fan

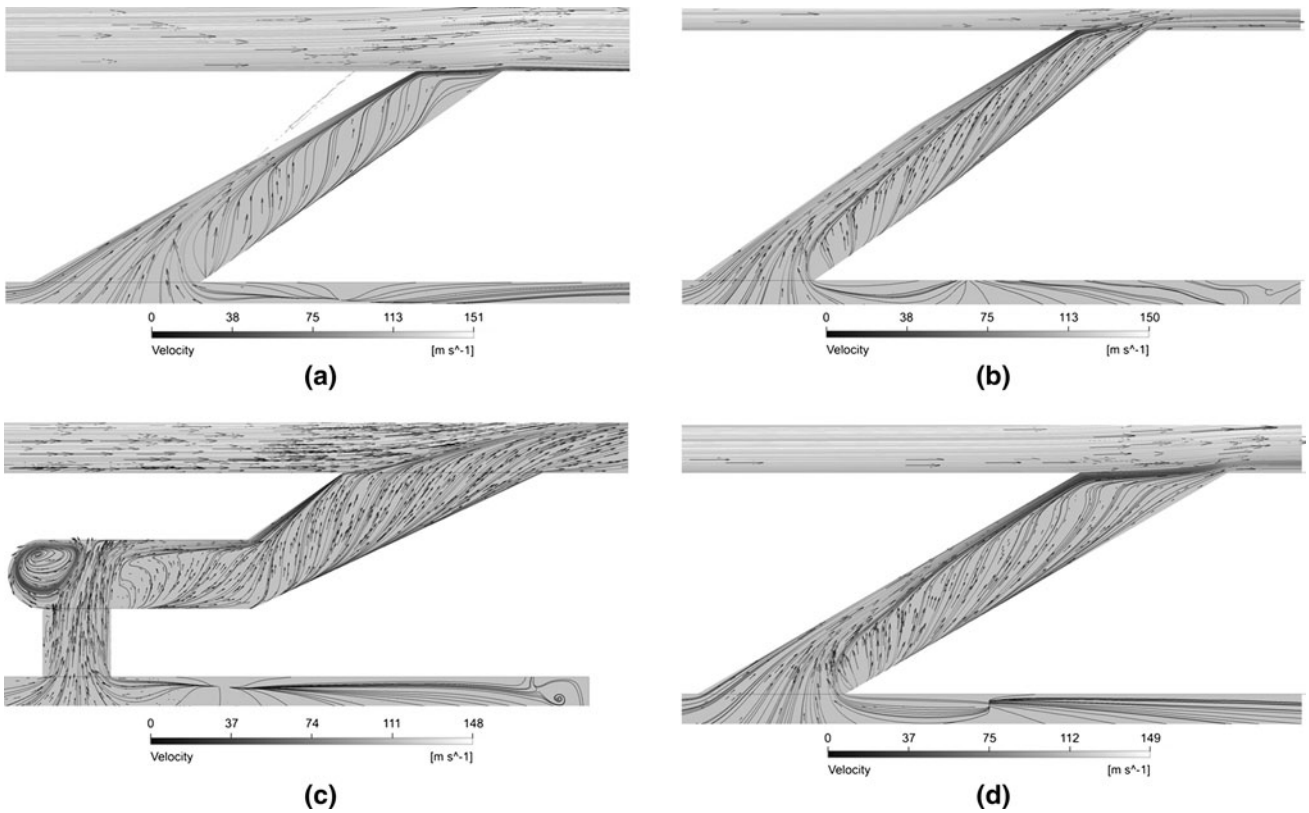

Fig. 10 The surface streamlines inside the hole (z = 0, y − x plane, M = 0.5): **a** crescent, **b** dumbbell, **c** louver, and **d** fan

the fan shaped hole has a single large diffuser while the dumbbell shaped hole has two small diffusers.

The streamlines of the coolant and velocity vectors on the y–z plane at x/D = 2 are presented in Fig. 11. These figures show how the flow develops after exiting the hole. All the shaped film-cooling holes generate a pair of vortices that is called the "kidney vortex" by impingement of coolant to the main stream. And, this is made from the spurting of coolant after it passes through the hole into the main stream. In the case of the crescent shaped hole, a couple of kidney vortices due to the coolant are located close to the cooling surface with distortion of the vortex shape, while the other holes make the kidney vortex more circular away from the wall than the crescent shaped hole. The louver shaped hole yields a distinctive vortex structure as compared to the others. By concentrating the coolant flow to the centerline of the cooling surface, the kidney vortices become close to each other. In the case of the dumbbell, fan, and crescent shaped holes, two pairs of vortices are observed after issuance from the hole. These are caused by interaction between the coolant flow and the main stream. As shown in Fig. 11, the outer vortices near the lateral end of hole are mainly generated by the coolant jet, while the inner vortices are produced by the main stream near the centerline where less coolant flows as compared to the outer region. As a result, higher film cooling effectiveness is found at the locations of the outer vortices.

Figure 12 shows how the kidney vortices develop downstream of the hole exit. In the case of the crescent and louver shaped holes, a couple of large kidney vortices are developed downstream of the hole, while two pairs of small vortices persist even far downstream of the hole in the case of the fan and dumbbell shaped holes. The crescent shaped hole has two branches of coolant which are more apart than those of other shaped holes. Therefore, this pair of vortices is made without the coolant. The dumbbell and fan shaped holes also have two branches of coolant, but differ from the crescent shaped hole. These shaped holes have one additional pair of vertices which is made by the coolant. There is a noticeable difference in the vortex structure between the crescent and louver holes. In the case of the crescent hole, the left vortex rotates clockwise while the right vortex rotates counterclockwise. This makes the two vortices apart, and the coolant spreads widely. On the contrary, in the case of the louver shaped hole, the vortices are made by the interaction between mainstream and coolant as shown in Fig. 12c, the left vortex rotates counterclockwise and the right vortex rotates clockwise, which makes the vortices closer.

The spatially averaged film-cooling effectiveness (η_s) is presented in Fig. 13. These values are averaged over an

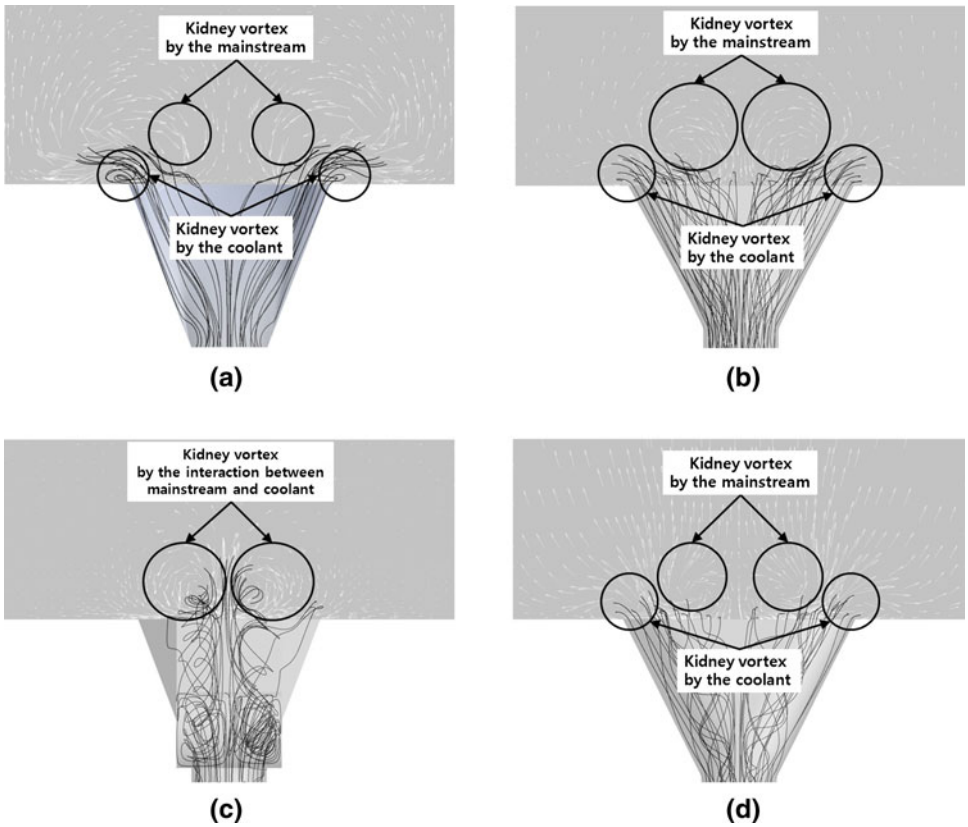

Fig. 11 The streamlines of the coolant and velocity vectors at the hole exit (x/D = 2, y–z plane, M = 1.0): **a** crescent, **b** dumbbell, **c** louver, and **d** fan

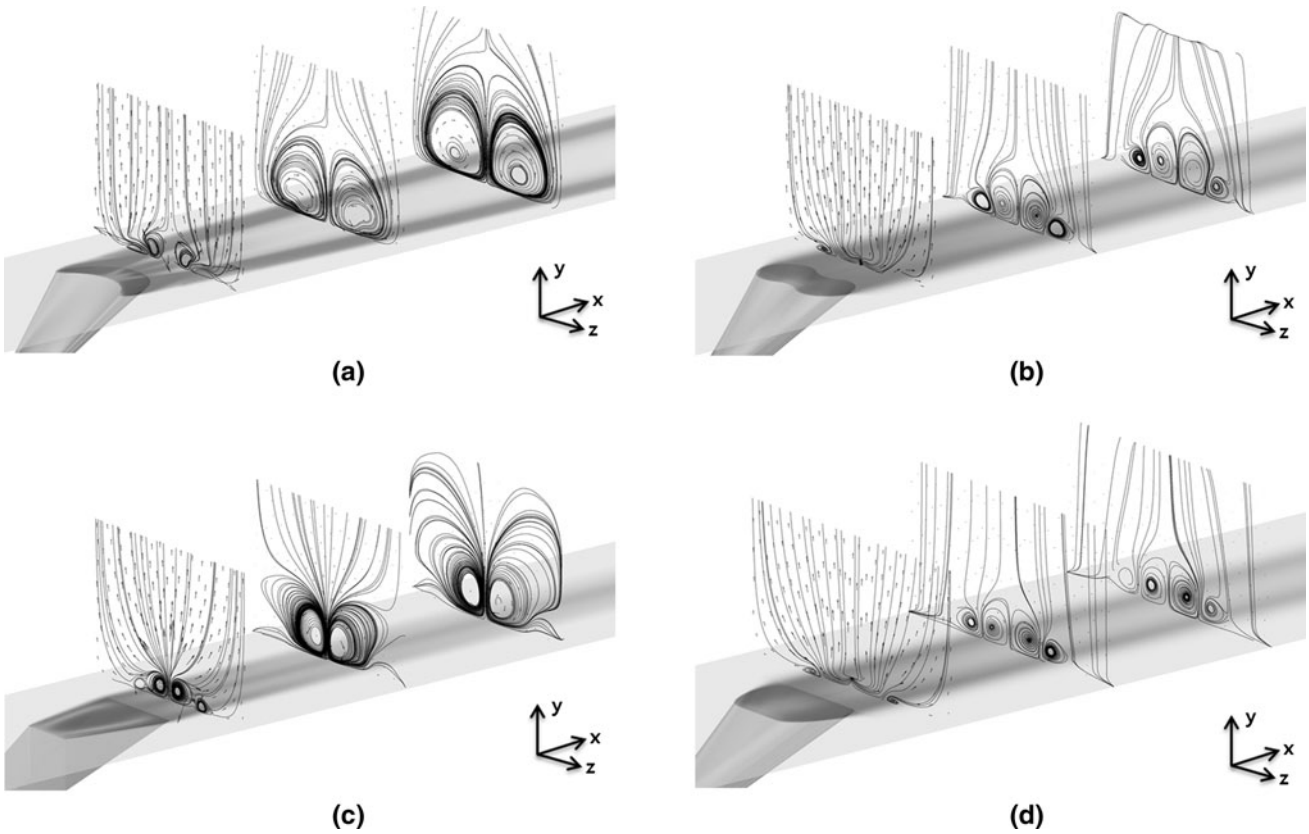

Fig. 12 The development of flow through surface streamlines and velocity vectors (x/D = 2, 7, 12, M = 1.0): **a** crescent, **b** dumbbell, **c** louver, and **d** fan

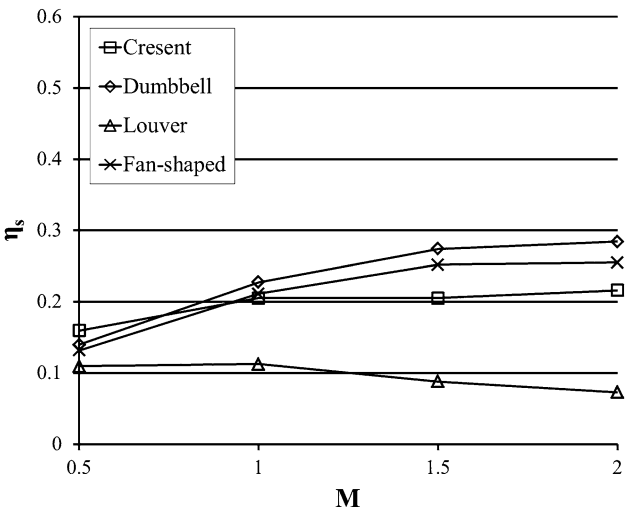

Fig. 13 The spatially averaged film-cooling effectiveness for various blowing ratios

area of 6 hole diameters in width and 20 hole diameters in length in the streamwise direction. The dumbbell shaped hole shows the highest film-cooling effectiveness for all the blowing ratios, while the louver shaped hole shows the lowest film-cooling effectiveness. And, the film-cooling effectiveness of the louver shaped hole decreases with the blowing ratio unlike in the other cases.

4 Conclusion

Evaluations of the film-cooling performance for various shapes of film-cooling hole at different blowing ratios have been performed. For the numerical analysis, three-dimensional Reynolds-averaged Navier–Stokes equations have been solved with the SST turbulence closure. The numerical results for the louver and fan shaped holes show good agreement with the experimental results. The film-cooling effectiveness has been analyzed for the crescent, dumbbell, louver, and fan shaped holes. In terms of the film-cooling effectiveness, the crescent hole yields higher film-cooling performance than the other holes at the blowing ratio of 0.5. But, with an increase in the blowing ratio, the dumbbell hole shows the highest film-cooling performance. The louver shaped hole shows the worst film-cooling performance for all the blowing ratios. It concentrates the coolant along the centerline downstream of the hole exit, but the crescent hole shows wide spreading of the coolant.

Acknowledgments This research was supported by the National Research Foundation of Korea (NRF) Grant No. 20090083510 funded by government (MEST) through the Multi-phenomena CFD Engineering Research Center.

References

1. Bunker RS (2005) A review of shaped hole turbine film-cooling technology. J Heat Transfer 127:441–453
2. Heidmann JD (2008) A numerical study of anti-vortex film cooling designs at high blowing ratio. Proceedings of the ASME Turbo Expo 2008, Berlin, GT2008-50845
3. Taslim ME (2004) Discharge coefficient measurements for flow through compound-angle conical holes with cross-flow. Int J Rotat Mach 10(2):145–153
4. Yiping Lu (2007) Effect of hole configurations on film cooling from cylindrical inclined holes for the application to gas turbine blades. Dissertation, Louisiana State University
5. Hyams DG, Leylek JH (2000) A detailed analysis of film cooling physics: part III—streamwise injection with shaped holes. J Turbomach Trans ASME 122(1):122–132
6. Liu JS, Malak MF, Tapia LA, Crites DC, Ramachandran D, Srinivasan B, Venkatramanan J (2010) Enhanced film cooling effectiveness with new shaped holes. Proceedings of ASME Turbo Expo 2010, Glasgow, GT2010-22774
7. Yu Y, Yen CH, Shih TIP, Chyu MK, Gogineni S (2002) Film cooling effectiveness and heat transfer coefficient distributions around diffusion shaped holes. J Heat Transfer 124(5):820–827
8. Ghorab MG (2010) An experimental investigation of a new hybrid film cooling scheme. Int J Heat Mass Transfer 53(21–22):4994–5007
9. Zhang XZ, Hassan I (2006) Film cooling effectiveness of an advanced-louver cooling scheme for gas turbines. J Thermophys Heat Transfer 20(4):754–763
10. Sargison JE, Guo SM, Oldfield MLG, Lock GD, Rawlinson AJ (2002) A converging slot-hole film-cooling geometry-part 1: low-speed flat-plate heat transfer and loss. J Turbomach Trans ASME 124(3):453–460
11. Nasir H, Acharya S, Ekkad S (2003) Improved film cooling from cylindrical angled holes with triangular tabs: effect of tab orientations. Int J Heat Fluid Flow 24(5):657–668
12. Lu YP, Dhungel A, Ekkad SV, Bunker RS (2009) Effect of trench width and depth on film cooling from cylindrical holes embedded in trenches. J Turbomach Trans ASME 131(1):1–13
13. Liu Cl, Zhu HR, Bai JT (2010) Film cooling performance of waist-shaped slot holes. Proceedings of ASME Turbo Expo 2010, Glasgow, GT2010-22237
14. CFX-11.0 Solver Theory (2006) ANSYS Inc
15. Menter F, Esch T (2001) Elements of industrial heat transfer prediction. 16th Brazilian Congress of Mechanical Engineering (COBEM), Uberlandia, Brazil
16. Wilcox DD (1986) Multiscale model for turbulent flows. AIAA 24th Aerospace Science Meeting, American Institute of Aeronautics and Astronautics
17. Saumweber C, Schulz A, Wittig S (2003) Free-stream turbulence effects on film cooling with shaped holes. J Turbomach 125:65–73
18. Launder BE, Sharma BI (1974) Application of the energy dissipation model of turbulence to the calculation of flow near a spinning disc. Lett Heat Mass Transfer 1(2):131–138
19. Vakhot V, Orszag SA, Thangam S, Gatski TB, Speziale CG (1992) Development of turbulence models for shear flows by a double expansion technique. Phys Fluids A 4(7):1510–1520